

# Structural Characterization of Magnetite and its Influence on the Formation of Composites with Polyaniline

Caroline Zanotto<sup>\*a</sup>, Fernando Ratuchne<sup>a</sup>, Eryza Guimarães de Castro<sup>a</sup>, and Patrícia Teixeira Marques<sup>b</sup>

<sup>a</sup>Chemistry Department, State University of Central West, Rua Simeão Varela de Sá 03, 85040-080, Guarapuava-PR, Brazil.

<sup>b</sup>Chemistry Department, Federal Technological University of Parana, Via do Conhecimento Km 01, 85503-390 Pato Branco-PR, Brazil.

*Article history:* Received: 15 April 2019; revised: 21 August 2019; accepted: 16 October 2019. Available online: 30 December 2019. DOI: <http://dx.doi.org/10.17807/orbital.v11i7.1403>

## Abstract:

In this paper, we present a simple and inexpensive method for synthesizing conductive polyaniline and magnetite composites. Firstly, the magnetite was synthesized by precipitation in basic medium from  $\text{FeCl}_3$ , and the Rietveld refinement confirmed the spinel structure. Different amounts of magnetite were used in the *in situ* synthesis of Pani- $\text{Fe}_3\text{O}_4$  composites to determine the influence, resulting in the following materials: Pani- $\text{Fe}_3\text{O}_4$  (1) with 0.06 g and Pani- $\text{Fe}_3\text{O}_4$  (2) with 0.24 g. The x-ray diffractogram demonstrates that interaction occurs between the polyaniline chains and the magnetite particles in the composites. Infrared and ultraviolet-visible vibrational spectra indicate that the composites are in the state of oxidation polyaniline salt emerald, which is the conductive form of greatest interest. Scanning electron microscopy images show that composites have particles with no definite geometry in the form of clusters, and the best homogeneity was achieved in the composite with the highest amount of magnetite. Evidence indicates that Pani- $\text{Fe}_3\text{O}_4$  (2) material with 0.24 g of magnetite to be incorporated in polyaniline synthesis may have more technologically interesting properties, but further studies will be needed for confirmation.


**Keywords:** conducting polymer; hybrid materials; iron oxide; metal oxide; Rietveld analysis

## 1. Introduction

Conductive polymers have a fascinating potential for technological applications, mainly due to their ability to combine chemical and mechanical properties of polymers with electronic properties of semiconductors and metals. For a long time, polymers were thought of only as materials with insulating applications, but now they are considered advanced materials that exhibit special functions in response to diverse external conditions, attracting attention to both research and innovation, making them intelligent materials [1]. These polymers have conjugated  $\pi$  bonds in their structure, which enables the process of conductivity due electron mobility.

Among the conductive polymers, Polyaniline (Pani) is one of the most studied polymers due to

its high conductivity, low monomer cost and wide variety of applications, electrochemical properties and ease of polymerization. However, Pani presents difficulties in processability, low electrochemical stability and change in volume during the electrochemical cycles, which results in low cycle stability in the oxidation and reduction process [2]. In order to overcome such structural instabilities of Pani, it is sought to produce composites that combine the properties of the conductive polymer with those of the metallic oxides. The stability of the Pani can be improved by allying the intrinsic properties of the polymer with particles of magnetite ( $\text{Fe}_3\text{O}_4$ ), which has specific and interesting properties from a technological point of view, obtained per the synergistic interaction between the organic and inorganic phases [3].

\*Corresponding author. E-mail:  [caroline.ztto@gmail.com](mailto:caroline.ztto@gmail.com)

Among the possible methods of synthesis, chemical precipitation is the most economically viable manner and provides good yield. The in-situ polymerization of the aniline in  $\text{Fe}_3\text{O}_4$  medium results directly in the conductive phase, emeraldine salt, emphasizing the versatility and ease of the method [4]. This method results in materials in the solid state, which is an important factor to provide the construction of films by the self-assembly technique [5], making electrodes and obtaining dispersions that favor a promising potential for further testing in characteristic applications such as sensors [6], supercapacitors, solar cells and more.

Per the incorporation of an inorganic material in the organic structure of the polymer, a composite is produced, increasing the semiconductor, mechanical and optical properties, being able to stabilize the material and making it interesting from a technological perspective [3]. For this reason, many researches are being carried out and many composites are being developed in the field of composite materials aiming at the most diverse applications [2, 7-9]. Metal oxides appear promising candidates for possessing rapid and reversible redox reactions and high capacitance [7, 9]. An example to be mentioned is the Pani- $\text{Fe}_3\text{O}_4$  composites, which through the exploration of the chemical, optical and magnetic properties, are being applied in solid phase extraction, chromatography [10], supercapacitors [11], thin films of nanohybrid Pani- $\text{Fe}_3\text{O}_4$  as corrosion protection [12], and electromagnetic devices, sensors, adsorption, magnetic separation [11, 13].

In this article, it was presented a study of the

effect of the incorporation of different amounts of  $\text{Fe}_3\text{O}_4$  in Pani, in order to investigate how these quantities interfere in forming the composite using morphological and structural characterization. The objective was to establish the best proportion of the inorganic phase to be used in forming the composite in order to produce materials to be applied on semiconductor devices

## 2. Results and Discussion

### 2.1 Structural characterization of magnetite

The X-ray diffractogram was studied by the Rietveld method and the results are presented in Figure 1-A. The characteristic diffraction peaks of magnetite in spinel structure can be observed. The peaks located at  $2\theta = 30.3^\circ$  (220);  $35.6^\circ$  (311);  $43.3^\circ$  (400);  $54.0^\circ$  (422);  $57.2^\circ$  (511);  $62.7^\circ$  (440), with their respective crystallographic planes are related to the spinel phase, confirming the presence of  $\text{Fe}_2\text{O}_3$  and FeO in the  $\text{Fe}_3\text{O}_4$  polycrystalline structure, in accordance with the diffraction indexes and values in literature [4, 14].

The refinement of the magnetite structure by the Rietveld method resulted in the following structural parameters:  $a = b = c = 8.37862 \text{ \AA}$  and residual statistics:  $R_p = 19.1$ ,  $R_{wp} = 23.6$ ,  $R_{exp} = 16.62$ ,  $\chi^2 = 2.02$ . The low intensity of the obtained error function (Difference) proves the quality of the structure refinement performed. The representation of the crystalline structure of the magnetite obtained after the refinement is indicated in Figure 1-B, where the tetrahedral and octahedral sites of the spinel structure are clearly observed.

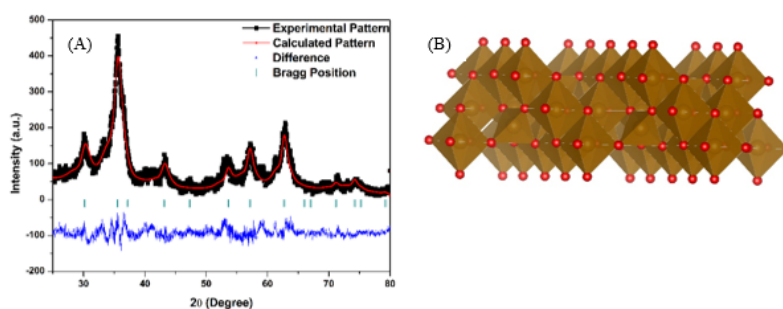


**Figure 1.** Experimental X-ray diffraction of the synthesized magnetite and the representation of the refinement by the Rietveld method (A) and the representation of the spinel structure of the magnetite (B).

In the UV-VIS spectrum observed in Figure 2-A, the band centered at 500 nm is highlighted. This band refers to the transition of electrons from the valence band (highest level of occupied energy HOMO) to conduction band (lowest level of unoccupied energy LUMO), which are characteristic of magnetite [15].

In the infrared vibrational spectrum, shown in Figure 2-B, the double band at 605  $\text{cm}^{-1}$  and 626  $\text{cm}^{-1}$  and the band at 890  $\text{cm}^{-1}$  are indicated. These are characteristics of the stretching interactions at the  $\text{Fe}_3\text{O}_4$  tetrahedral and octahedral Fe-O sites and at 1621  $\text{cm}^{-1}$  for the Fe-O bond vibrations. Other bands present in the region of 797  $\text{cm}^{-1}$ , 460  $\text{cm}^{-1}$  and 402  $\text{cm}^{-1}$  of the spectrum refer to vibrations and symmetrical and asymmetrical stretching of the material, being consistent with spectra reported in the literature for the pure magnetite [4, 16].

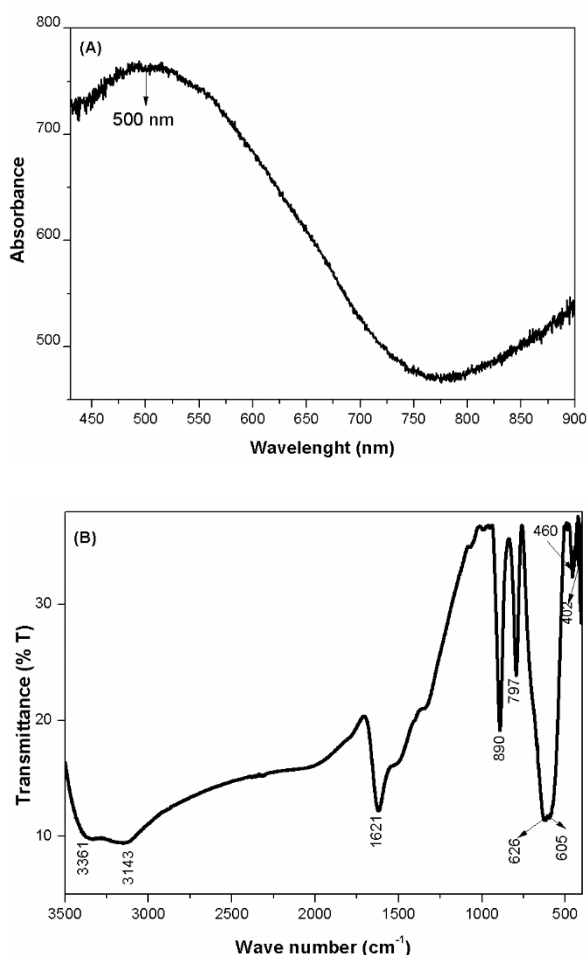


**Figure 2.** A) UV-VIS spectrum in solid and B) spectrum in the infrared region of the synthesized magnetite.

Figure 3 presents the images obtained by scanning electron microscopy of the magnetite, which indicate that the particles have spherical morphology in the form of agglomerates in the micrometric scale (greater than 30  $\mu\text{m}$ ).

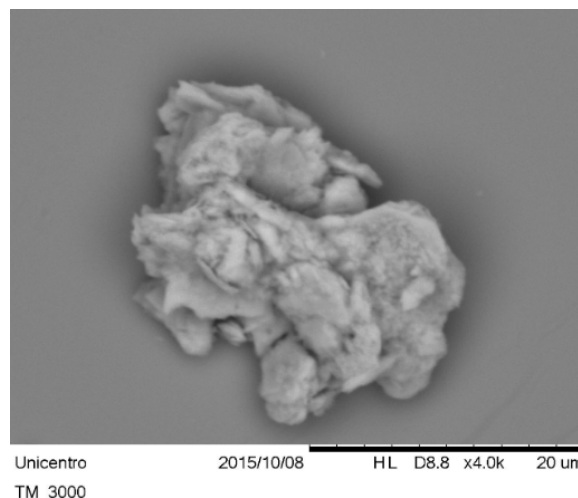


**Figure 3.** SEM image for  $\text{Fe}_3\text{O}_4$ .

### 3.2. Characterization of composites

In Figure 4, the X-ray diffractograms are represented, where the peaks in Pani- $\text{Fe}_3\text{O}_4$  (1) are: 25° and 35° and in Pani- $\text{Fe}_3\text{O}_4$  (2): 25.5°, 35.5°, 43° and 57° in  $2\theta$ , corresponding to the planes (200), (311) and (200), (311), (400), (511) of the magnetite, respectively. These peaks and indexations correspond to the interaction between the spinel phases of  $\text{Fe}_3\text{O}_4$  and the Pani. Not all the peaks present in the magnetite were observed in the hybrid, since Pani is crystalline and its peaks are wider covering a larger area at  $2\theta$ , covering some of them. This suggests that there was interaction between the organic and inorganic phases in the composite formation. The intensity of the peaks varied with the amount of magnetite incorporated in the hybrid, and there was a better interaction for Pani- $\text{Fe}_3\text{O}_4$  (2) hybrid material with 0.24 g of magnetite, which presented better interaction between phases, having higher peaks. Evident, higher crystallinity [4].

Figure 5-A shows the UV-VIS spectra with emphasis on the 641 band in the Pani- $\text{Fe}_3\text{O}_4$  (1) composite, attributed to the presence of electronically excited polarons and transition between the ligand and antiligand orbitals  $\pi - \pi^*$  of quinoids rings and the band at 435 nm assigned to the polarons- $\pi^*$  radical transition cation of the Pani chains [17]. In the Pani- $\text{Fe}_3\text{O}_4$  (2) composite,

obtained with the highest amount of  $\text{Fe}_3\text{O}_4$ , these bands have absorption maximums at 649 nm and 445 nm that can be attributed to a doping extension due to polymer protonation polarons [18]. These characteristics confirm the presence of relocated polarons, which makes the mobility of load carriers greater in composite materials [19]. A more extended band may also represent interactions of polyaniline quinoid rings with  $\text{Fe}_3\text{O}_4$  present in the magnetite structure [13, 20].

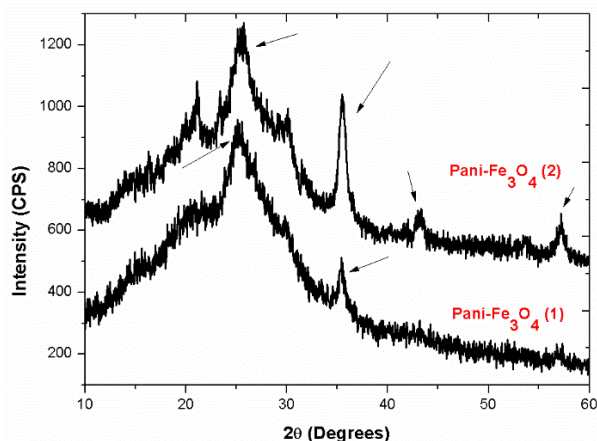


**Figure 4.** X-ray Diffractograms of composites Pani- $\text{Fe}_3\text{O}_4$  (1) with 0.06 g and Pani- $\text{Fe}_3\text{O}_4$  (2) with 0.24 g of  $\text{Fe}_3\text{O}_4$ .

In the infrared vibrational spectra shown in Figure 5-B, the interactions between the polymer and magnetite phases in the spectrum region between  $510$  and  $1293\text{ cm}^{-1}$ , which refer to the Fe-O bond vibrations with bands, are highlighted. Fe-O interaction characteristics interspersed with the polymer chains. In the region of  $1137\text{ cm}^{-1}$  in Pani- $\text{Fe}_3\text{O}_4$  (1) and  $1149\text{ cm}^{-1}$  in Pani- $\text{Fe}_3\text{O}_4$  (2) there is a C=N stretch of polyaniline, in the region between  $1594 - 1495\text{ cm}^{-1}$ , presence of  $\pi$ -links displaced by protonation of the polymer. Other absorptions in the region of  $2800\text{ cm}^{-1}$  and  $2900\text{ cm}^{-1}$  are attributed to the elongations of the C-H chains and in the region of  $3000\text{ cm}^{-1}$  assigned to water molecules bound in the polymer chain [2, 4, 16]. Authors such as [4] report that composites with higher amounts of magnetite may present higher absorption intensity, which was not observed in this case.

The SEM images obtained for the hybrid materials are presented in Figure 6, where the inorganic and crystalline phase appears as regions of major contrast and well defined in

composite Pani- $\text{Fe}_3\text{O}_4$  (2), greater dispersibility of the magnetite particles in the polymer matrix, where they are in higher amounts, than in Pani- $\text{Fe}_3\text{O}_4$  (1), where greater agglomerates are observed.

These quantities of magnetite (0.06 g and 0.24 g) were chosen by previous studies and literature results to estimate the most appropriate amount of magnetite in proportion to the polymer in order to obtain better physicochemical properties, thus optimizing the synthesis route of the composite.

Considering that studies indicate that there is a maximum amount of magnetite that the chains of a conjugated polymer can incorporate, therefore, large amounts of magnetite can act as obstacles to the electronic transfer between the polyaniline chains, decreasing the active area of the hybrid, highlight the importance of this study in synthesis optimization [21].

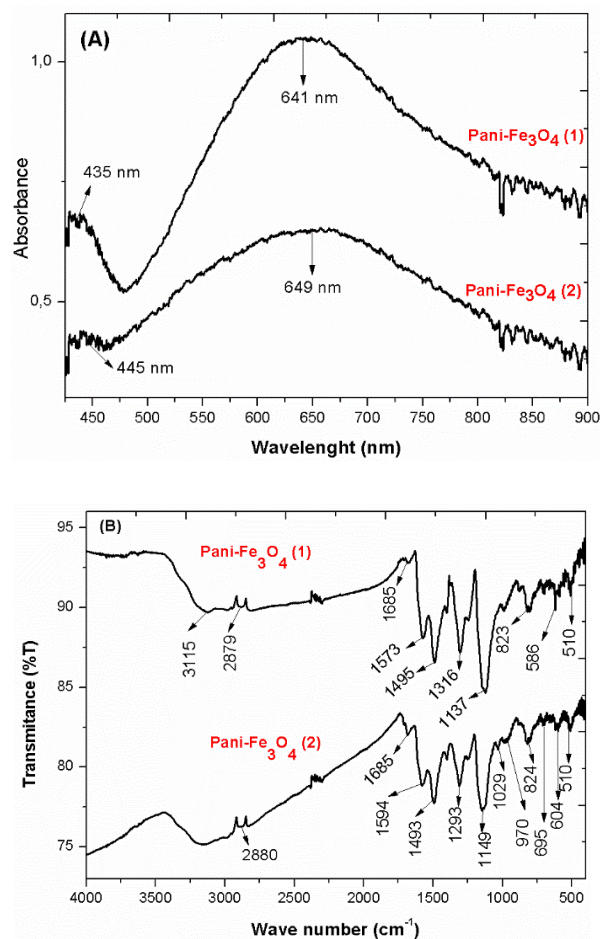


**Figure 5.** (A) spectra in the UV-VIS and (B) infrared regions for the composites Pani- $\text{Fe}_3\text{O}_4$  (1) with 0.06 g and Pani- $\text{Fe}_3\text{O}_4$  (2) with 0.24 g of  $\text{Fe}_3\text{O}_4$ .

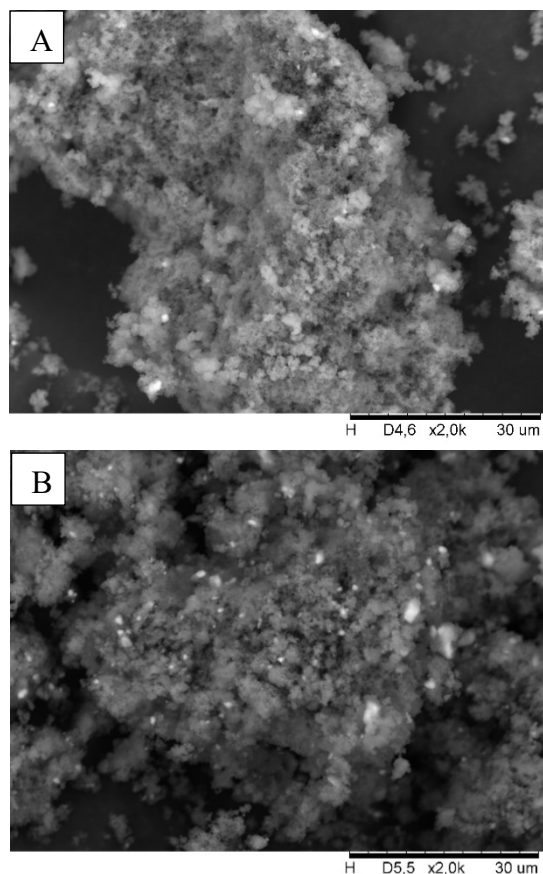


**Figure 6.** SEM for (A) Pani-Fe<sub>3</sub>O<sub>4</sub> (1) and (B) PAni-Fe<sub>3</sub>O<sub>4</sub> (2) composites.

Some factors that influence this amount of magnetite that have been incorporated can be cited: magnetite particle size, doping level, length of conjugation and bonding in the Pani chains and molecular orientation. Above this ideal quantity, there is no improvement, or in some cases even worsens the characteristics of the composite over the precursor. In the literature, authors such as [22] evaluated the influence of iron (oxide) content on conductivity in composites formed between polymers such as polypyrrol or polyaniline and magnetite as inorganic phase and concluded that with increasing magnetite content, conductivity values up to 40% by weight when it reaches a maximum value. Above this percentage becomes less effective as the amount of iron increases.

### 3. Material and Methods

All reagents used were from Sigma-Aldrich with high purity. Two composites with different amounts of the oxide were synthesized; (Pani-Fe<sub>3</sub>O<sub>4</sub> (1) with 0.06 g and Pani-Fe<sub>3</sub>O<sub>4</sub> (2) with 0.24 g) by the following methodologies:

**Synthesis of Fe<sub>3</sub>O<sub>4</sub>:** The synthetic route was carried out by chemical precipitation of FeCl<sub>3</sub> in basic medium, using 7.5 mL of a 2 mol L<sup>-1</sup> iron (III) chloride solution, to which 5 mL of a 1 mol L<sup>-1</sup> Na<sub>2</sub>SO<sub>3</sub> solution was slowly added under stirring. To this system, 10 mL of 25% v/v NH<sub>4</sub>OH were added, keeping the system under stirring for 30 min. Thereafter, the precipitate formed was decanted by magnetic separation and washed, discarding the supernatant. The solid sample was dried at room temperature, macerated and stored in a desiccator for use in the synthesis of the composites.

**Synthesis of Pani-Fe<sub>3</sub>O<sub>4</sub> composites:** 100 mL of 1 mol L<sup>-1</sup> HCl and 0.30 g of the oxidizing agent (NH<sub>4</sub>)<sub>2</sub>S<sub>2</sub>O<sub>8</sub> were mixed under stirring. Then, 1 mL of the previously distilled aniline monomer and the solid Fe<sub>3</sub>O<sub>4</sub> (0.06 g or 0.24 g) synthesized above were added, keeping the system under stirring for 5 h, yielding the Pani-Fe<sub>3</sub>O<sub>4</sub> (1) or Pani-Fe<sub>3</sub>O<sub>4</sub> (2). After this period, the solids were centrifuged, washed, dried and stored in a desiccator for characterization.

X-ray diffraction analyzes were performed on a Rigaku Miniflex 600 equipment with a voltage of 40 Kv and a 15 mA current at a scanning rate of 2°/minute and range of 10 to 60 degrees in 2θ. The representation of the magnetite structure was carried out using Vesta software version 3.2.1 [23] and the Spectrum refinement was performed in Fullprof software [24]. The ultraviolet-visible (UV-Vis) electron spectra were obtained with an Ocean Optics spectrophotometer, model USB2000, equipped with tungsten lamp and silicon / germanium detectors (UV-Vis, 350-900 nm), connected through optical fiber and operating in diffuse reflectance mode. Infrared vibration spectra (FTIR) were obtained using a Shimadzu Prestige-21 spectrophotometer, in the range of 4000-400 cm<sup>-1</sup>, with samples in the form of KBr pellets in transmission mode. Scanning Electron Microscopy (SEM) images were obtained with the Hitachi TM3000 coupled to EDS SNIPTED 3000 analyzer.

### 4. Conclusions

The method of obtaining the magnetite proved to be a cheap, simple route that results in high purity material, as proved by the refinement of the X-ray diffractogram by the Rietveld method. The

composite showed good yield and ease of obtaining.

From the characterization results and the literature, there is some evidence to indicate that the Pani-Fe<sub>3</sub>O<sub>4</sub> (2) hybrid with 0.24 g of incorporated magnetite showed the highest synergistic interaction between the phases, confirmed by infrared spectra and XRD, in which there were characteristic interactions that corroborate that the inorganic phase is found between Pani structures in a more orderly manner. These results suggest that there is greater mobility of cargo carriers and a tendency to be better drivers, which makes it interesting for technological applications.

For a better definition of the ideal mass ratio of magnetite to be used as an inorganic phase, other studies with mass quantities in g between the proportions 0.06 and 0.24 g are suggested to broaden the analysis of the results, as well as other studies, auxiliary characterization techniques

## Acknowledgments

To the central analysis of UTFPR Campus Pato Branco.

## References and Notes

- [1] Zhao, Q.; Qi, J.H.; Xie, T. *Progr. Polym. Science*, **2015**, 49-50, 79. [\[Crossref\]](#)
- [2] Li, Y.; Zheng, Y. *J. Appl. Polym.* **2018**, 135, 46103. [\[Crossref\]](#)
- [3] Fleaca, C. T.; Dumitrache, F.; Morjan, I.; Niculescu, A. M.; Sandu, I.; Ilie, A.; Stamatina, I.; Iordache, A.; Vasile, E.; Prodan, G. *Appl. Surface Science* **2016**, 374, 213. [\[Crossref\]](#)
- [4] Umare, S. S.; Shambharkar, B. H.; Ningthuojam, R. S.; *Synth. Met.* **2010**, 160, 1815. [\[Crossref\]](#)
- [5] Das, M.; Sarkar, A. A. D. *Synth. Met.* **2019**, 249, 69. [\[Crossref\]](#)
- [6] Zhu, W.; Jiang, W.; Xu, L.; Li, B.; Zhou, C. *Anal. Chem. Acta* **2015**, 886, 37. [\[Crossref\]](#)
- [7] Megha, R.; Ravikiran, Y. T.; Chethan, B.; Rajprakash; H. G.; Vijayakumari, S. C.; Thomas, S. *J. Mater. Sci: Mater Electron.* **2008**, 29, 7253. [\[Crossref\]](#)
- [8] Subramanian, E.; Santhanamari, P.; Murugan C. *J. Electron. Mater.* **2018**, 47, 4764. [\[Crossref\]](#)
- [9] Fu, W.; Zhao, E.; Ren, X; Magasinski, A.; Yushing, G. *Adv. Energy Mater.* **2018**, 8, 1703454. [\[Crossref\]](#)
- [10] Yang, X.; Qiao, K.; Ye, Y.; Yang, M.; Li, J.; Gao, H.; Zhang, S.; Zhou, W.; Lu, R. *Anal. Chim. Acta* **2016**, 934, 114. [\[Crossref\]](#)
- [11] Eftekhari, A.; Li, L.; Yang, Y. *J. Power Sources* **2017**, 347, 86. [\[Crossref\]](#)
- [12] Bagherzadeh, M.; Haddadi, H.; Iranpour, M. *Prog. Org. Coat.* **2016**, 101, 149. [\[Crossref\]](#)
- [13] Zanotto, C.; Ratushne, F.; Melquiades, F. L.; Marques, P. T.; De Castro, E. G. *Rev. Virtual Quim.* **2017**, 9, 2494. [\[Crossref\]](#)
- [14] Guo, J.; Gu, H.; Wei, H.; Zhang, Q.; Li, Y.; Yonug, D. *P. J. Phys. Chem.* **2013**, 117, 10191. [\[Crossref\]](#)
- [15] Cornell, M. R.; Schwertmann, U. The iron oxide. Structure, properties, reactions, occurrences and uses. 2<sup>nd</sup> ed. Editora Wiley-Vch, 2003.
- [16] Birsan, C.; Predoi, D.; Andronescu, E. *J. Optoelectron. Adv. Mater.* **2007**, 9, 1821. [\[Link\]](#)
- [17] Castro, E. G. D.; Zarbin, A. J. G.; Oliveira, H. P.; Galembeck, A. *Synth. Met.* **2004**, 146, 57. [\[Crossref\]](#)
- [18] Costa, C. R.; Souza, F. G.; *Polim.* **2014**, 24, 243. [\[Crossref\]](#)
- [19] Tabares, B. E. J.; Isaza, F. J.; Torresi, S. I. C. *Mater. Chem. Phys.* **2012**, 132, 529. [\[Crossref\]](#)
- [20] Huang, J.; Li, Q.; Li, D.; Wang, Y.; Dong, L.; Xie, H.; Wang, J. *Langmuir* **2013**, 29, 10223. [\[Crossref\]](#)
- [21] Chen, A.; Wang, H.; Zhao, B.; Li, X. *Synth. Met.* **2003**, 139, 411. [\[Crossref\]](#)
- [22] Qui, G.; Wang, Q. *Macromol. Mater. Eng.* **2005**, 291, 68. [\[Crossref\]](#)
- [23] Momma, K.; Izumi, F. *J. Appl. Crystallogr.* **2011**, 44, 1272. [\[Crossref\]](#)
- [24] Rodrigues-Carvajal, J. Fullprof: a program for Rietveld refinement and pattern matching analysis. In: Satellite Meeting on Powder Diffraction, 15, 1990, Toulouse. Abstracts. [s.l.] : IUCr, 1990. p. 127.